Study for performance of thermo-optic matrix switches with flexible switching units and Banyan networks

De-Gui Sun
Wenyuan Deng
Shulin E
Ying Zha
Zhiying Liu
Xiaoqi Li
Chinese Academy of Sciences
State Key Laboratory of Applied Optics
Changchun Institute of Optics
Fine Mechanics and Physics
16 East Nanhu Street
Changchun, JL 130031
China
E-mail: deguisun_b@yahoo.com

Abstract. A large-scale optical matrix switch is generally composed of a permutation of switching units connected by a network of optical signal paths. In this work, a configuration of optical matrix switches with flexible switching units and Banyan networks is proposed. With Banyan networks, silica-based waveguides, and two types of switching units, the insertion loss of the optical matrix switch configuration is extensively studied for serial scales from 2×2 to 64×64. Typically for an 8×8 optical matrix switch, the insertion losses are achieved 3.0 dB for a rearrangeably nonblocking configuration with two-state 2×2 switching units, and 4.7 dB for a strictly nonblocking configuration with three-state 2×2 switching units when the intersection angle is designed as 30 deg. Even at the released intersection angle of 20 deg, the insertion losses of 4.0 and 5.8 dB can be achieved for the rearrangeably nonblocking and strictly nonblocking configurations, respectively. In addition, the blocking property and the scalability of the large-scale matrix optical switches with this regime are analyzed. [DOI: 10.1117/1.2158997]

Subject terms: optical matrix switch; Banyan network; optical waveguide interconnection; two-state switching unit; three-state switching unit; insertion loss; blocking property; scalability.

Paper 040691R received Oct. 1, 2004; revised manuscript received Apr. 13, 2005; accepted for publication Jun. 8, 2005; published online Jan. 24, 2006.

1 Introduction

With the active development and applications of communication systems, integrated optics represent a promising approach in these advanced optical information areas.[1,2] A new trend to search and develop relevant passive and active components requires advanced optoelectronic technologies to produce Si-based photonic devices for optical waveguide interconnects.[2,3] Among all the passive and active components in optical communication and processing systems, the optical space switches are key components. In particular, research and development of high-performance silica-based waveguide thermo-optic switches attain many accomplishments, because the thermo-optic waveguides fit the requirements of either small-scale advanced switching devices or large-scale integrated matrix switches.[4–8] In particular, some silica-based devices have met the basic requirements of industrial systems as design and fabrication of planar lightwave circuit (PLC) technologies are gradually approaching maturation.[4–6] The great progress in waveguide thermo-optic switches shows an exciting essence in low-speed operations because of their ultra-low loss, mature fabrication, physical stability, and feasibility of batch production.[6–8] Thermo-optic waveguide devices can also be built with other materials such as crystals and polymers. For instance, polymer-based thermo-optic waveguide switches have their inherent advantages, including low-speed operations, because of ultra-low power consumption for switching operations and great flexibility in fabrication and processing.[9,10]

Large-scale matrix switches are required to meet the increasing switching capacity in optical communications and processing. The main characteristics of a large-scale optical matrix switch include blocking characteristics, insertion loss, power consumption, device size, response speed, scalability, and cross talk. With PLC technologies, the strategy for implementing a high-performance large-scale optical matrix switch is an effective combination of a network of optical signal paths and a permutation of switching units, including 2×2 and 1×2 switches, which are referred to as nodes of the network. In this case, the characteristics include the blocking property, insertion loss, power consumption, and ease of fabrication with PLC technology are of importance. In this work, two types of 2×2 switching units and Banyan interconnection networks are studied to constitute nonblocking and low-loss thermo-optic matrix switches with silica-based PLC technologies. Then, the influences of the intersection angles among the waveguide links and the excess loss of the Mach-Zehnder interferometer (MZI) units on the performance of silica-based waveguide thermo-optic matrix switches based on this regime are studied, and the insertion loss of systems is discussed. Finally, the blocking property and the scalability of the matrix switches based on this configuration are analyzed.

2 Design of Devices

A 1×2 or 2×2 optical switch can be directly employed either as an individual optical switching device or as a switching unit to build the matrix switches. When a 1×2 or 2×2 optical switch is used as an individual optical switching device or as a switching unit to build low-count matrix switches, cross talk is a critical concern. When it is used as a switching unit to build high-count matrix switches, more important issues are optical loss, operating power consumption, device size, and scalability rather than cross talk. In the past decade, waveguide thermo-optic switches mainly involve two mechanisms, one is based on the MZI structure as 1×2 or 2×2 switching units[4–8] and the other is based on a digital thermo-optic effect to produce 1×2 or 2×2 switching operations,[8–10] which is referred to as a digital optical switch (DOS). MZI configuration and the DOS structure do not matter; however, the operating rules are important for a switching unit in large-scale matrix switches. These rules determine the operating processes of systems and directly impact major characteristics of optical matrix switches such as the blocking property and the insertion loss of the system with an effective construction of network. We know, unlike the electronic signals, that two or more photonic signals can pass through one another without any cross talk, unless the intersection angle of these signal paths is too small, so the blocking property should be directly occurring at the node of the network when two optical signals are simultaneously passing through this node rather than from the links.

To analyze the dependence of a matrix switch blocking property on the operating rules of the 2×2 switching units that are used as nodes of the network, we first assume two cases of 2×2 switching operations: one is that the 2×2 switching operations are simultaneously controlled; and the other is that the 2×2 switching operations are separately controlled. More exactly, the first type of 2×2 switching unit is only based on a single modulating effect for two input optical signals to choose two output states, and is referred to as a two-state 2×2 switching unit. The second type of 2×2 switching unit is based on four separate modulating effects for two input optical signals to choose three output states, and is referred to as a three-state 2×2 switching unit.

2.1 *Two-State* 2×2 *Switch*

A two-state 2×2 switch is schematically represented in Fig. 1(a). Its basic operating principle is that an input optical signal can only have two options for outputs: ports 1 and 2. For the case of two input optical signals, once a signal is determined to choose one of the two output ports by either having an outside modulating effect or not having an outside modulating effect, the other one has been determined to choose the other output port simultaneously, because this type of 2×2 switch only has two output ports. The switching operations between the input ports and the output ports can be summarized in Fig. 1(b). Therefore, this type of 2×2 switch is referred to as a two-state switch. Note that the operations of the two-state 2×2 switch can totally have two combinations and the switching operations for two input signals can be controlled by one modulating

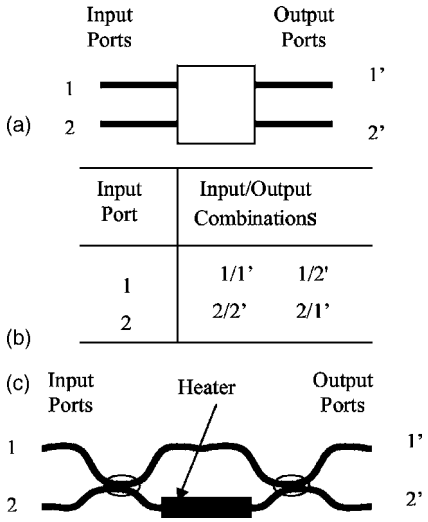

Fig. 1 Two-state 2×2 switch: (a) symbol and concept; (b) summary of operating states for the two input signals; and (c) the typical MZI-based structure.

effect. To implement this type of two-state 2×2 switch with PLC technologies, the typical MZI-based structure is shown in Fig. 1(c).

2.2 *Three-State* 2×2 *Switch*

A three-state 2×2 switch is schematically represented in Fig. 2(a). Its basic operating principle is that an input optical signal can have three options for outputs: two output ports 1 and 2, and one end 0 (the stopping state). For the case of two input optical signals, after a signal has been determined by having an outside modulating effect to choose one of two output ports, the other one still has two options for its outputs. One option is determined to choose the other output port by having another outside modulating

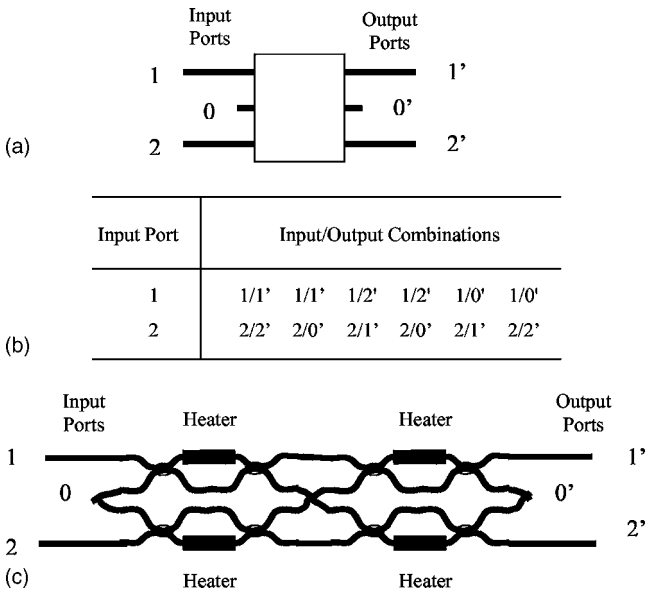

Fig. 2 Three-state 2×2 switch: (a) symbol and concept; (b) summary of operating states for the two input signals; and (c) the typical MZI-based structure.

effect, and the other option is to choose the stopping state without any outside modulating effect. The switching operations between the two input ports and two output ports can be summarized in Fig. 2(b), and the switching operations for two input signals can be controlled by four separate modulating effects. Thus, this type of 2×2 switch is referred to as a three-state switch. Note that the operations of a three-state 2×2 switch can totally have six combinations, and the switching operations for two input signals have to be controlled by four separate modulating effects. By comparing the three-state 2×2 switch with the two-state switch, the three-state 2×2 switch has three times more operations for two input signals than the two-state one, which is very helpful for reducing blocking probability of the system at this node and simplifying the construction of a network. To implement this type of three-state 2×2 switch with PLC technologies, the typical MZI-structure-based three-state 2×2 switch is shown in Fig. 2(c). Note that the three-state 2×2 switch relies on two separate modulating effects, as mentioned before.

3 Analysis for Banyan Network Property

Research on optical interconnections with PLC technologies has been becoming more and more significant as the capacities of optical processing and communication systems increase. In PLC-based optical interconnections, the regular optical interconnection for constituting the networks of optical signal paths is one of the focuses of research, because it not only reduces the complexity of implementation systems, the difficulty of controlling systems, the circuit depth (levels), and the blocking probability, but also improves the uniformity of optical loss. In particular, research today on silica-based waveguide optical interconnections has become one of the widely acceptable PLC technologies in integrated optoelectronic and photonic communications and information processing systems. The regular interconnection for the networks of optical signal paths is more significant.

The perfect shuffle, the crossover, and the butterfly are commonly used for interconnecting array processors, permutation networks, and sorting.[11–13] Figures 3(a)–3(c) are the schematic constructions of the perfect shuffle, the crossover, and the butterfly, respectively, where k indicates the starting nodes and k' indicates the receiving nodes. It can be easily noticed from Fig. 3(a) that the linking lines, which indicate the optical signal paths, are not parallel to one another in the perfect shuffle interconnection. It can be noticed from Fig. 3(b) that half of the optical signal paths are parallel to one another and the other half are not in the crossover interconnection. These parallel linking lines are the straight links from the starting nodes to the receiving ones, and all the unparallel linking lines have one intersection point. It can be noticed from Fig. 3(c) that in the butterfly interconnection, the optical signal paths can be categorized into three groups, and in each group all the optical signal paths are parallel to one another. It turns out that although the perfect shuffle, the crossover, and the butterfly are topologically equivalent, they differ from one another in both architectures and optical implementation approaches.[12–14] The butterfly interconnection is demonstrated to have the most regular construction and is most suitable for optical implementation, including PLC and free-space optical technologies.[12–17] For the one-stage butterfly network with a width of N, as shown in Fig. 3(c), there are two fan-in lines or two fan-out lines at each node, one is a straight interconnect line and the other is a butterfly interconnect line. If k indicates the address number of the nodes on the input end, we define the address numbers of the nodes of the straight and butterfly interconnect lines as k'_s and k'_b $(k'_s, k'_b = 0, 1, \ldots, N-1)$, respectively, on the output end, which gives the following relations:

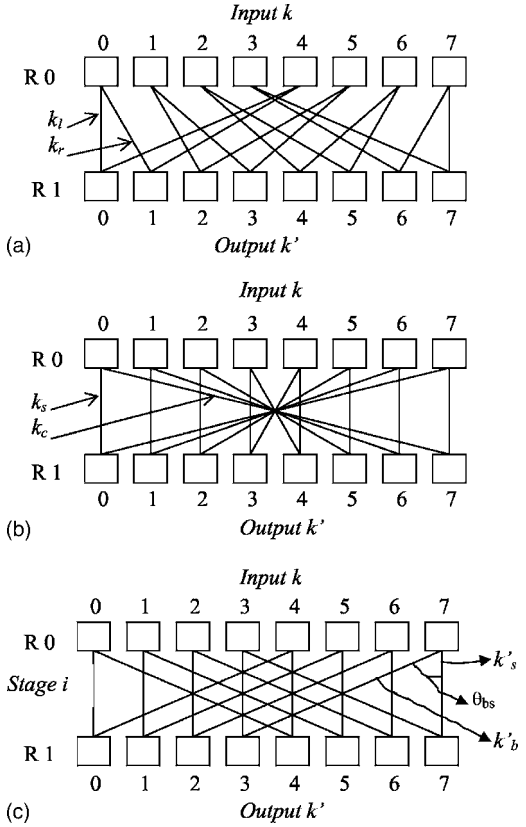

Fig. 3 Construction of three typical interconnections for building Banyan networks: (a) perfect shuffle; (b) crossover; and (c) butterfly.

$$k'_s = k \rightarrow (k = 0, 1, \ldots, N-1), \tag{1}$$

$$k'_b = \begin{cases} k + N/2 \rightarrow (k < N/2) \\ k - N/2 \rightarrow (N/2 \leqslant k < N). \end{cases} \tag{2}$$

To analyze the construction feature of butterfly interconnection for the Banyan networks, let us define $\delta = k' - k$, which represents the interconnect angles of link lines from the input end to the output end.

For the butterfly network, we obtain, from Eqs. (1) and (2)

$$\delta_s = k'_s - k = 0 \rightarrow (k = 0, 1, \ldots, N-1), \tag{3}$$

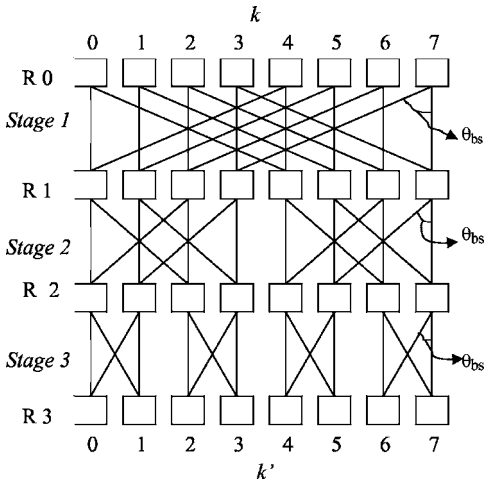

Fig. 4 Construction and concept of the Banyan network with a width of $N=8$ and the butterfly interconnection.

$$\delta_b = k_b' - k = \begin{cases} N/2 \rightarrow (k < N/2) \\ -N/2 \rightarrow (N/2 \leqslant k < N). \end{cases} \quad (4)$$

Note from Eqs. (3) and (4) that not only the interconnect angles of the straight interconnect lines (δ_s), but also those of the butterfly interconnect lines (δ_b) in one group ($k=0,\ldots,N/2-1$ or $k=N/2,\ldots,N-1$), are independent of the number of address nodes k; that is, not only all the straight interconnect lines but also the butterfly interconnect lines in one group are parallel, which is also easy to see in Fig. 3(c). As represented in Fig. 4, the butterfly interconnection can be used to constitute a Banyan network with PLC technologies. If the width of a Banyan network is N, the number of link stages is n, and there is a relation of $N=2^n$ in the network ($N=8$ and $n=3$ in Fig. 4). The link interconnection patterns often include sizes N, $N/2$, $N/4$, etc. at the stage of 1, 2, and 3, respectively.[11,12] It is easy to see from Fig. 4 that an N-wide Banyan network contains $(n+1)N$ nodes (i.e., the switching units in the PLC-based optical matrix studied in this work), and as shown in Fig. 4, the $n+1$ rows of nodes are successively labeled with $R\,0, R\,1, \ldots, R\,n$. The number of nodes in the network indicates the hardware cost of the optical matrix switch based on this network.

As discussed earlier, the Banyan network with the butterfly interconnection is the most regular of these three typical interconnections in terms of construction, because not only all the angles of the straight interconnect lines (δ_s) but also those of the butterfly interconnect lines (δ_b) are independent on the number of address nodes k, which shows that all the butterfly interconnect lines in one group, like the straight interconnect lines, are parallel. This property of Banyan networks with butterfly interconnections is similar to that of manipulator networks and is easily extended to higher level structures for more advanced applications.[13–16] Particularly, the combination of PLC and micro-optical technologies in 3-D forms can make the Banyan-network-based optical switching systems possess more important functions for more significant applications.[15–17] Thus, optical waveguide implementation of butterfly interconnect networks can be completed under parallel waveguide channels with the same length and interconnection angle. The butterfly interconnection is, therefore, a better approach in integrated photonic devices with PLC technologies.

4 Simulation and Optimization of Performance

A large-scale optical matrix switch is composed of a permutation matrix of switching units connected by a network of signal paths. A 2×2 switch can be employed as a switching unit, so low insertion loss and low power consumption are two critical performance characteristics, since they directly impact the scalability of this switching unit. Silica has a low thermo-optic coefficient ($\partial n/\partial T \sim +1.1\times10^{-5}K^{-1}$)[8], but silica-based waveguides have an ultra-low propagation loss, so they are suitable for the requirements of large-scale optical matrix switches using MZI-based configuration as switching units.[5–7] In particular, in the past decade, many more endeavors to increase the scale of silica-based waveguide thermo-optic switches for industrial applications and to reduce the power consumption of the switching unit have been made, and a power consumption of less than 150 mW for a 2×2 switch is achieved.[5–7]

4.1 *Study for Insertion Loss*

For PLC-based optical interconnection networks, an intersection of two or more waveguide channels can cause an optical loss, and it is referred to as an intersection-induced loss. As we discussed in Sec. 3, in a Banyan network with a width of N, as shown in Fig. 4, all the butterfly interconnect lines have the same interconnection angle with all the straight lines at the same stage of network. Note from Fig. 4 that there are two intersection angles and three intersection scenarios in the Banyan network with the butterfly interconnection. Two intersection angles are: 1. the angle between a butterfly link and a straight link and 2. the angle between two butterfly links. These two intersection angles are referred to as θ_{bs} and θ_{bb}, respectively. It is obvious that $\theta_{bs}=\theta_{bb}/2$. Three intersection scenarios include: 1. the intersection of two butterfly links and a straight link; 2. the intersection of a butterfly link and a straight link; and 3. the intersection of two butterfly links. The intersection-induced losses in these three scenarios are expressed as $L_{\text{inter}}(\theta_{bs}/\theta_{bs})$, $L_{\text{inter}}(\theta_{bb})$ and $L_{\text{inter}}(\theta_{bs})$, respectively. As shown in Fig. 4, at the i'th stage, each butterfly link has an intersection with each of the $N/2^i-1$ straight links at the intersection angle of θ_{bs}, namely, there are $N/2^i-1$ intersections at the angle of θ_{bs}. Each $N/2^i$ butterfly link in one direction group has an intersection with each $N/2^i$ butterfly link in the other direction group, and half of these intersections (i.e., $N/2^{i+1}$) overlap with the previous intersections at the angle of θ_{bs}, and the other half do not. Thereby, if $n_{\text{inter}}(\theta_{bs}/\theta_{bs})$, $n_{\text{inter}}(\theta_{bb})$, and $n_{\text{inter}}(\theta_{bs})$ indicate the numbers of the first, second, and third scenarios of intersections, respectively, as discussed before in terms of the construction of the Banyan networks with the butterfly interconnection, they can be calculated by

$$n_{\text{inter}}(\theta_{bs}/\theta_{bs}) = \begin{cases} \dfrac{N}{2^{i+1}} & \text{for } i = n-1 \\ 0 & \text{for } i = n, \end{cases} \tag{5}$$

$$n_{\text{inter}}(\theta_{bb}) = \frac{N}{2^i} - n_{\text{inter}}(\theta_{bs}/\theta_{bs}), \tag{6}$$

$$n_{\text{inter}}(\theta_{bs}) = \frac{N}{2^i} - 1 - n_{\text{inter}}(\theta_{bs}/\theta_{bs}). \tag{7}$$

Thus, for these three scenarios of intersections among waveguide channels as optical signal paths in networks, the angle-dependent intersection-induced losses of an optical signal should be expressed as

$$L_{\text{inter}}(\theta_{bs}/\theta_{bs}) = L(\theta_{bs}/\theta_{bs}) \cdot n_{\text{inter}}(\theta_{bs}/\theta_{bs}), \tag{8}$$

$$L_{\text{inter}}(\theta_{bb}) = L(\theta_{bb}) \cdot n_{\text{inter}}(\theta_{bb}), \tag{9}$$

$$L_{\text{inter}}(\theta_{bs}) = L(\theta_{bs}) \cdot n_{\text{inter}}(\theta_{bs}). \tag{10}$$

Thereby, for the $N \times N$ scale optical waveguide matrix switch based on an n-stage Banyan network with butterfly interconnection, the total intersection-induced losses for the prior three intersection scenarios can be calculated by Eqs. (11)–(13), respectively, as

$$TL_{\text{inter}}(\theta_{bs}/\theta_{bs}) = \sum_{i=1}^{n} L_{\text{inter}}(\theta_{bs}/\theta_{bs}), \tag{11}$$

$$TL_{\text{inter}}(\theta_{bb}) = \sum_{i=1}^{n} L_{\text{inter}}(\theta_{bb}), \tag{12}$$

$$TL_{\text{inter}}(\theta_{bs}) = \sum_{i=1}^{n} L_{\text{inter}}(\theta_{bs}). \tag{13}$$

Finally, with the consideration of all the angles, the total intersection-induced loss of an optical signal is

$$TL_{\text{inter}} = TL_{\text{inter}}(\theta_{bs}/\theta_{bs}) + TL_{\text{inter}}(\theta_{bb}) + TL_{\text{inter}}(\theta_{bs}). \tag{14}$$

For silica-based waveguides, we select the cross section waveguide size as $5.5 \times 5.5\ \mu\text{m}^2$, and the refractive index difference is 0.75%. Then, the propagation loss is $L_{\text{prop}} = 0.04$ dB/cm and the waveguide-fiber coupling loss is $L_{\text{WFC}} = 0.25$ dB/*po*int.[4] These two sources of optical loss in silica-based waveguide devices have been commercially acceptable. Thus, for optical matrix switches with the regime studied in this work, the excess loss of the switching units is the other structure-dependent source of optical loss besides the intersection-induced loss, so it is important to study. In the regime of optical matrix switches studied in this work, the MZI-based 2×2 switches are employed as switching units, so the excess loss L_{MZI} of the MZI configuration is one of the major sources of optical loss. For the $N \times N$ optical waveguide matrix switch based on an n-stage Banyan network with butterfly interconnection, the total excess loss of switches is represented as

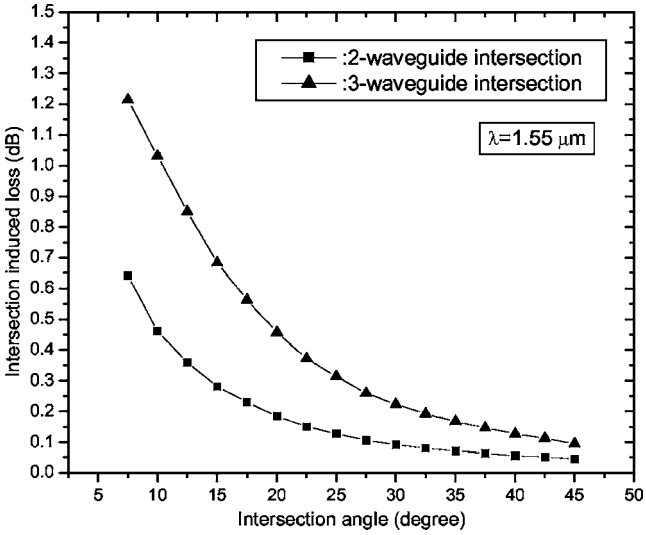

Fig. 5 Simulation results of the intersection-induced optical loss versus the intersection angle θ_{bs} with respect to two scenarios: (a) the loss induced by the two-line intersection $L_{\text{inter}}(\theta_{bs})$ and (b) the loss induced by the three-line intersection $L_{\text{inter}}(\theta_{bs}/\theta_{bs})$.

$$TL_{\text{switch}} = m(n+1)L_{\text{MZI}}, \tag{15}$$

where the integer m is the state factor of a 2×2 switching unit used in the system, $m=1$ for systems using the two-state 2×2 switches, and $m=2$ for systems using three-state 2×2 switches.

In this work, we mainly study and simulate the two main sources of optical loss: the intersection-induced loss among waveguide links and the excess loss of switching units. With the commercial software tool of the Optiwave Corporation at Ottawa, Ontario, Canada, OptiBPM, we first simulate the intersection-induced losses at $\lambda = 1.55\ \mu$m with respect to the intersection scenarios of θ_{bs} and θ_{bs}/θ_{bs}, and obtain $TL_{\text{inter}}(\theta_{bs})$ and $TL_{\text{inter}}(\theta_{bs}/\theta_{bs})$ versus the intersection angle, as shown in Fig. 5. Note that the intersection losses for these two intersection scenarios quickly decrease with the intersection angle, which is of paramount importance in large-scale PLC based optical matrix switches. The typical values of the intersection-induced losses are $TL_{\text{inter}}(\theta_{bs}) = 0.18$ dB, $TL_{\text{inter}}(\theta_{bs}/\theta_{bs}) = 0.45$ dB, and $TL_{\text{inter}}(\theta_{bb}) = 0.06$ dB at $\theta_{bs} = 20$ deg; and $TL_{\text{inter}}(\theta_{bs}) = 0.09$ dB, $TL_{\text{inter}}(\theta_{bs}/\theta_{bs}) = 0.22$ dB, and $TL_{\text{inter}}(\theta_{bb}) \approx 0$ dB at $\theta_{bs} = 30$ deg. For the other main source of optical insertion loss of the system, we simulate the excess loss L_{MZI} of an MZI unit versus the wavelength in C-band (1.525 to 1.575 μm) with respect to three typical structures of 3-dB couplers used in the MZI configuration, and obtain the wavelength-dependent relations of the excess loss of an MZI configuration for these three 3-dB coupler structures, as shown in Fig. 6. Note from Fig. 6 that the optical excess loss of the MZI configuration is insensitive to wavelength, and the stable value is $L_{\text{MZI}} = 0.40$ dB.

As a summary, the sources of inducing the insertion loss of the optical matrix switch include: 1. intersections of waveguide links, 2. excess losses of switching units, 3. the

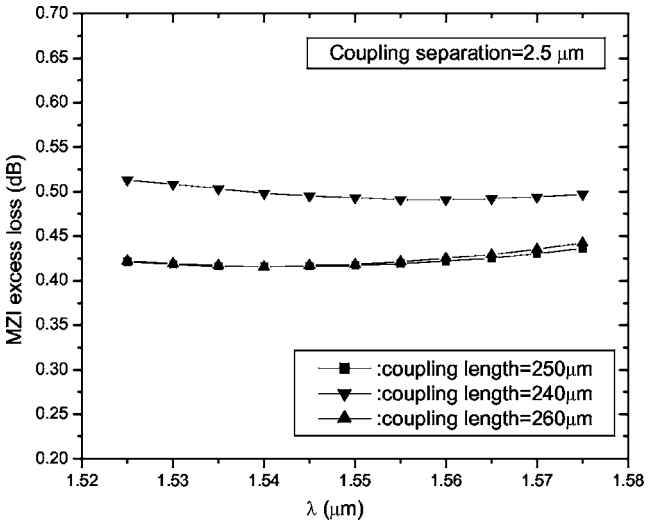

Fig. 6 Simulation results for the dispersion of the switching-unit excess loss with respect to three different coupling lengths.

propagation loss of waveguide material, and 4. waveguide-fiber coupling losses. To study the influence of the intersection scenarios of waveguide links on the optical loss in this regime, we further simulate the total intersection-induced loss TL_{inter} and its three components: $TL_{\text{inter}}(\theta_{bs}/\theta_{bs})$, $TL_{\text{inter}}(\theta_{bb})$, and $TL_{\text{inter}}(\theta_{bs})$ with Eqs. (5)–(13), and obtain the relations between the intersection-induced losses of the system and the number of network stages at $\theta_{bs}=20$ deg and $\theta_{bs}=30$ deg, as shown in Figs. 7(a) and 7(b), respectively. What we need to claim is that the number n of stages and the width N of the network is related by $N=2^n$, namely, the values of n: 1, 2, 3, 4, 5, 6 correspond to the values of N: 2, 4, 8, 16, 64. Note that the total intersection-induced loss at $\theta_{bs}=20$ deg is higher than that at $\theta_{bs}=30$ deg by more than two times, and $TL_{\text{inter}}(\theta_{bs}/\theta_{bs})$ is always the biggest contribution and $TL_{\text{inter}}(\theta_{bb})$ is the smallest contribution to the total intersection loss TL_{inter} at both the typical angles of $\theta_{bs}=20$ deg and $\theta_{bs}=30$ deg.

Assuming the l_{MZI} is the averaged length of one MZI-based switching unit and that L_{prop} indicates the propagation loss of the silica-based waveguides, the total propagation loss of the system can be expressed as

$$TL_{\text{prop}} = m(n+1)l_{\text{MZI}} \cdot L_{\text{prop}}. \tag{16}$$

Finally, we obtain the insertion loss IL of the matrix optical switch as

$$IL = TL_{\text{inter}} + TL_{\text{switch}} + 2L_{\text{WFC}} + TL_{\text{prop}}. \tag{17}$$

By taking the commercially acceptable values $L_{\text{prop}}=0.04$ dB/cm of propagation loss of silica-based waveguides and the waveguide-fiber coupling loss $L_{\text{WFC}}=0.25$ dB/*po*int, the values of intersection-induced losses obtained in the previous simulation at the intersection angles of 20 and 30 deg the excess loss of switching units of $L_{\text{MZI}}=0.42$ dB, and with Eqs. (5)–(16), we obtain simulated results of the insertion loss IL and its three major components, including the total intersection-induced loss TL_{inter}, the total excess loss TL_{switch} of switching units, and

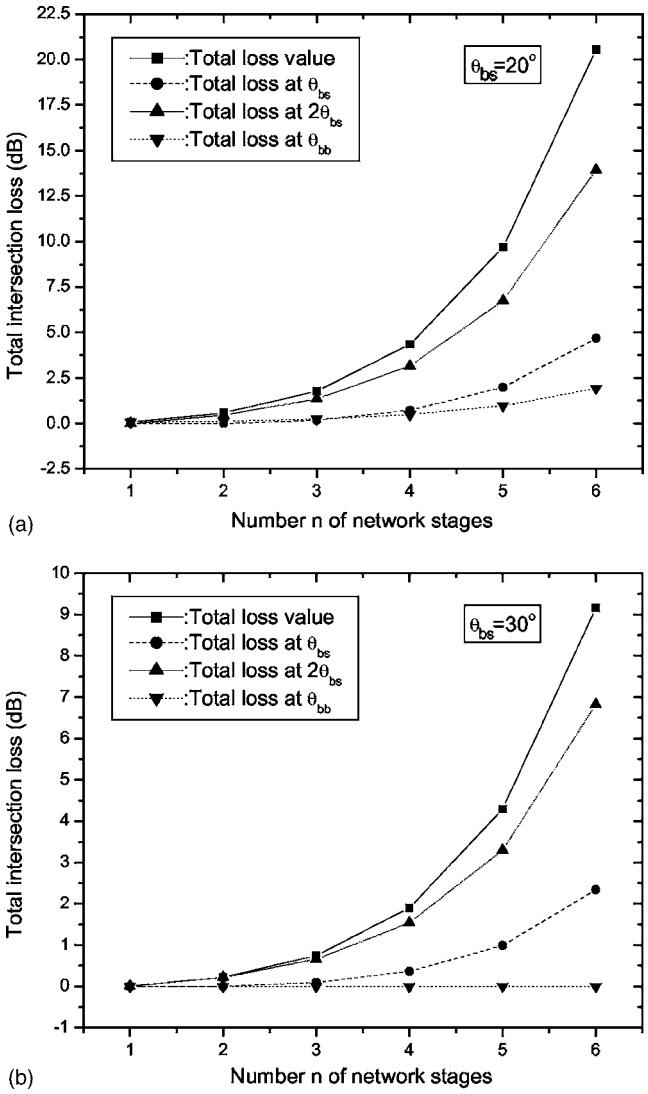

Fig. 7 Simulation results of the total intersection-induced loss and three main intersection sources versus the stage number of networks with respect to two intersection angle values: (a) $\theta_{bs}=20$ deg and (b) $\theta_{bs}=30$ deg.

total propagation loss TL_{prop} as functions of the stage numbers of the network at $\theta_{bs}=20$ deg and $\theta_{bs}=30$ deg, as shown in Figs. 8(a) and 8(b), respectively. Note that the intersection-induced loss is the biggest contribution to the insertion loss IL of the matrix switches studied in this work and quickly increases with the size of the matrix switches. In the same manner as TL_{inter} shown in Fig. 7, the insertion loss at $\theta_{bs}=20$ deg is higher than that at $\theta_{bs}=30$ deg by more than two times. By combining the two intersection angles $\theta_{bs}=20$ deg and $\theta_{bs}=30$ deg with the two types of switching units, the two-state 2×2 switch and the three-state 2×2 switch, we further obtain simulated results of the insertion loss IL of optical matrix switches based on the silica waveguides and the Banyan network with butterfly interconnection as functions of the number n of stages with respect to four different cases, as shown in Fig. 9. Note that the insertion loss of an optical matrix switch using two-state 2×2 switching units is really lower than the one us-

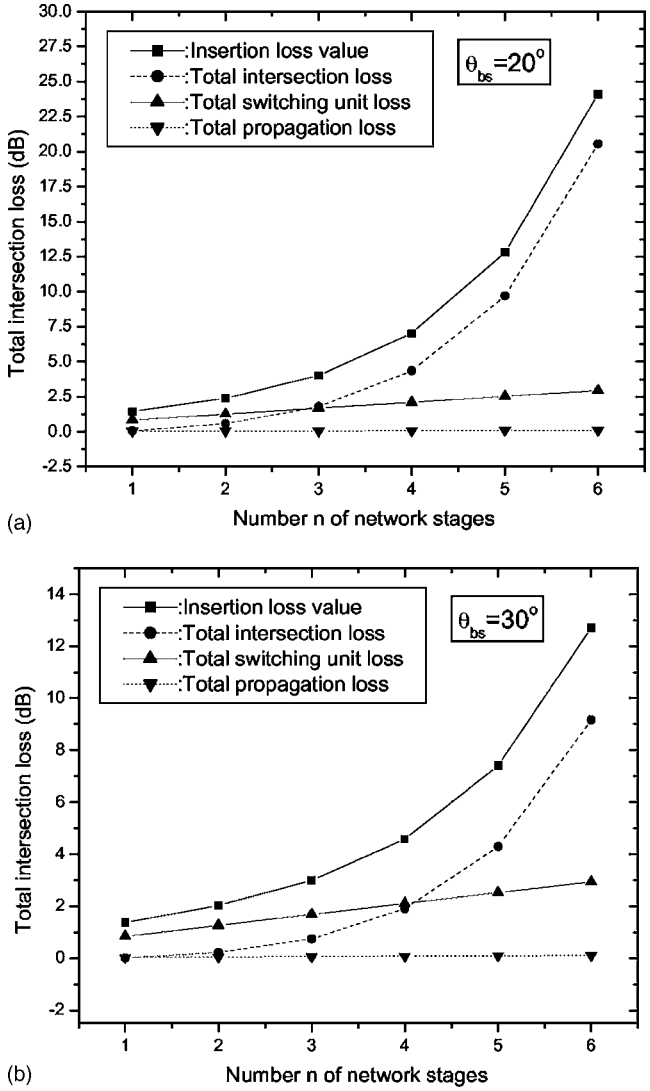

Fig. 8 Simulation results of the total insertion loss and main loss sources of optical matrix switches with a Banyan network and silica waveguides versus the stage number of networks: (a) θ_{bs}=20 deg; and (b) θ_{bs}=30 deg.

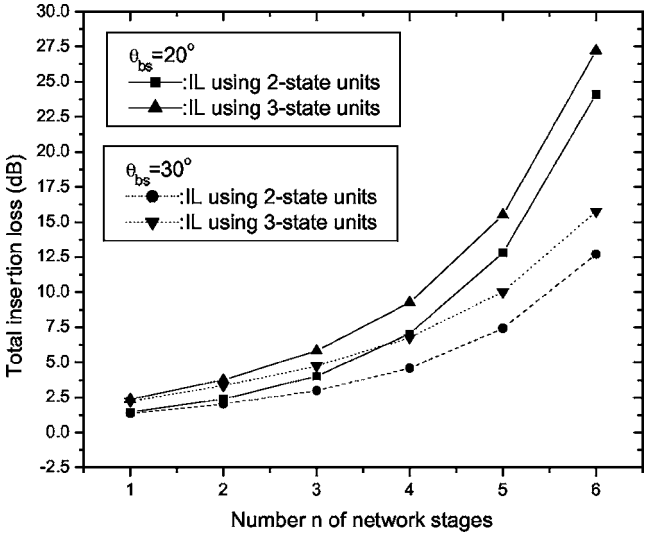

Fig. 9 Insertion losses of system versus stage number of the Banyan network with respect to the four combinations of two θ_{bs} values and two types of switching units.

ing three-state 2×2 switching units, which is the reason the blocking performance of the former is worse than the latter. For low insertion loss, the best case is the system using the intersection angle θ_{bs}=30 deg and the two-state switching units. But, as analyzed later, the system size of the optical matrix switches using θ_{bs}=30 deg is bigger than that using θ_{bs}=20 deg, and designing the system is more difficult. Also, the matrix switches using three-state switching units should be strictly nonblocking, while those using two-state switching units should be rearrangeably nonblocking. Namely, there is a tradeoff between the insertion loss and the blocking property in the regime of optical matrix switches discussed in this work.

4.2 *Analysis for Blocking Property*

The blocking property of a communication network means that when some signal links are active, the active links probably block other links being activated.[18,19] As we know, the Banyan network is constructed in terms of subnetworks as $N/2^i$. This construction rule can help us find the characteristics of the network, including the blocking property. By taking a look at the construction of the 8×8 Banyan network shown in Fig. 4, we find that if an optical signal from an input port k is directed to its destination k', all its passing-through switching units are active. The switching units at the input row (row 0) and output row (row 3) cannot block other signals communications, and only the active switching units at rows 1 and 2 have blocking probabilities to other signals. It is easy to see that an active switching unit at column 1 has two input ports related to it, so it probably blocks one signal. But, an active switching unit at column 2 has three input ports related to it, so it probably blocks two signals. Thus, the rule for determining the blocking probability of this system can be defined by

$$I_b = \left(\frac{N}{2} - k\right)\sum_{i=1}^{n-2} i. \tag{18}$$

The network distribution in space only has signal communications in space, so the blocking in this network only occurs in space. To solve the blocking problem, the switching operations of each switching unit can be time division multiplexing.[18] In this scheme, a time-division-slot clock is defined and employed to cover all the possible blocked optical signals. Each time slot has two parts: the duration T_d, where data are present, and the duration T_g, where the guard band is set for transmission and synchronization margin. If T_{ts} is the duration of one time slot, this time slot is defined by

$$T_{ts} = T_d + T_g. \tag{19}$$

Then, the duration of a frame can be represented as

$$T_f = I_b \cdot T_{ts}. \quad (20)$$

Finally, the nonblocking property of optical matrix switches with the time-division-multiplexing scheme is actually to rearrange the optical signal to another route in time and thus is rearrangeably nonblocking.[4] A time-division multiplexing scheme will require circuit-switched applications, so it is not the main content of this work.

What we discuss here is the other approach to solve the blocking problem. As discussed in Sec. 2, this approach is to extend the switching unit from the two-state 2×2 switch to the three-state switch, as discussed earlier. If the MZI structure is employed to implement the three-state 2×2 switch shown in Fig. 2(c), the number of MZI units for one switching unit is two, thereby the excess loss will be doubled, even more than two times that of the two-state switching unit, as it has a relatively more complicated structure, as discussed before. Operating power consumption will be doubled compared to that using two-state switching units. However, in accordance with the simulated results, the insertion loss is still acceptable, at least it is less than the doubled value of that of using two-state switching units. More importantly, optical matrix switches with three-state switching units can be nonblocking without a need for other routes, including the time-division-multiplexing scheme, so this kind of nonblocking property is referred to as strictly nonblocking.[2,4,19]

4.3 *Analysis for Scalability*

Scalability of a scheme for matrix switches is one important evaluation standard.[3] It is used to evaluate the essence of extending to the large-scale matrix switches, so there are several aspects in a scheme of matrix switches to impact the scalability. These aspects include optical loss, power consumption, size of the switching units, the manufacturability, and the configuration of the matrix switches. The scheme for silica-based optical waveguide matrix switches is proposed and investigated. With wide investigation in both the structure of the system and the components such as switching units and construction used in the system, the insertion loss performance of optical matrix switches with this scheme is much better than other similar PLC-based systems. These advantages represent one aspect of the scalability of optical matrix switches. In addition, two types of switching units are defined and introduced into the optical matrix switches, so the exchangeability between conditional nonblocking and strictly nonblocking structures becomes possible, as discussed in Sec. 4.2. Blocking cannot happen at the switching units in both the starting row and the receiving row. As in Fig. 4, the switching units in these two rows are all the 1×2 switches in the prior discussion. After the 1×2 starting switching units and the 2×1 switching receiving units were replaced with three-state 2×2 switches,[19] the switch scales doubled without decrease in the original system performance. This merit of this scheme represents the other aspect of the scalability of optical matrix switches.

5 Conclusion

A new configuration of large-scale optical waveguide matrix switches using the Banyan network with butterfly interconnection and flexible switching units is proposed and investigated. Main characteristics of performance, insertion loss, scalability, and blocking property, are discussed. This process of building large-scale optical matrix switches mainly has two advantages: low insertion loss and nonblocking properties. In this regime, the Banyan network with silica-based PLC technologies is employed and two types of 2×2 switch units are used: the two-state and three-state 2×2 switches are introduced, and the influence of the type of 2×2 switch unit on both the insertion loss and blocking property is analyzed. The construction of the Banyan network with butterfly interconnection used in this regime is widely studied. With analyses and simulation for the insertion loss of the silica-based optical 8×8 matrix switches, the insertion losses of 3.0 and 4.7 dB are achieved for the conditionally nonblocking scheme with respect to the intersection angles of 20 and 30 deg, respectively, and 4.0 and 5.8 dB for the strictly nonblocking scheme, respectively. Then, the main sources of the insertion loss of the system are extensively studied. Particularly, the losses induced by intersections among waveguide links and the excess loss of the switching units are numerically simulated and discussed. Further, approaches for solving the blocking characteristics of the optical matrix switches using Banyan networks and PLC-based butterfly optical interconnection technologies are concluded to have essential applications in optical matrix switches. Finally, the scalability of the configuration for silica-based optical waveguide matrix switches is discussed. For optical matrix switches using two-state switching units, the rearrangeably nonblocking property is implemented with a time-vision-multiplexing scheme for switching operations. For optical matrix switches using three-state switching units, the strict-sense nonblocking property is implemented without the time-division-multiplexing scheme for switching operations.

Acknowledgment

This work is supported by the 100-Person-Plan Foundation of the Chinese Academy of Sciences.

References

1. R. Ramaswami and K. N. Sivarajan, *Optical Networks: A Practical Perspective*, Morgan Kaufmann Publisher, New York (1998).
2. S. J. McNab, N. Moll, and Y. A. Vlasov, Ultra-low loss photonic integrated circuit with membrane-type photonic crystal waveguides," *Opt. Express* **11**(12), 2927–2939(2003).
3. G. I. Papadimitriou, C. Papazoglou, and A. S. Pomportis, "Optical switching: switch fabrics, techniques, and architectures," *J. Lightwave Technol.* **21**(2), 384–405 (2003).
4. T. Miya, "Silica-based planar lightwave circuits: passive and thermal active devices," *IEEE J. Sel. Top. Quantum Electron.* **6**(1), 38–45 (2000).
5. R. Kasahara, M. Yanagisawa, T. Goh, A. Sugita, A. Himeno, M. Yasu, and S. Matsui, "New structure of silica-based planar lightwave circuits for low-power thermooptic switch and its application to 8 $\times$8 optical matrix switch," *J. Lightwave Technol.* **20**, 993–1000 (2002).
6. M. P. Earnshaw, J. B. D. Soole, M. Cappuzzo, G. E. Laskowski, and A. Paunescu, "8$\times$8 optical switch matrix using generalized Mach-Zehnder interferometers," *IEEE Photonics Technol. Lett.* **15**(6), 810–812 (2003).
7. T. Goh, M. Yasu, K. Hattori, A. Himeno, M. Okuno, and Y. Ohmori, "Low-loss and high-extinction-ratio silica-based strictly nonblocking 16$\times$16 thermooptic matrix switch," *IEEE Photonics Technol. Lett.* **10**(6), 358–360 (1998).
8. M. Hoffmann, P. Kopka, and E. Vogas, "Thermo optical digital switch arrays in silica-on-silicon with defined zero-voltage state," *J. Lightwave Technol.* **16**(3), 395–400 (1998).

9. W. Y. Huang, M. C. Oh, H. M. Lee, H. Park, and J. J. Kim, "Polymeric 2×2 switch consisting of asymmetric Y-junctions and Mach-Zehnder interferometer," *IEEE Photonics Technol. Lett.* **9**, 761–763 (1997).
10. M. C. Oh, H. J. Lee, M. H. Lee, J. H. Ahn, and S. G. Han, "Asymmetric X-junction thermooptic switches based on fluorinated polymer waveguides," *IEEE Photonics Technol. Lett.* **10**, 813–815 (1998).
11. M. J. Murdocca, A. Huang, J. Jahns, and N. Streil, "Optical design of programmable logic arrays," *Appl. Opt.* **27**(9), 3155–3160 (1988).
12. D. G. Sun, Q. Xiang, N. X. Wang, Z. Weng, and J. Feng, "Butterfly interconnection implementation for an n-bit parallel full adder/subtractor," *Opt. Eng.* **31**(7), 1568–1575 (1992).
13. T. J. Cloonan, "Topological equivalence of optical crossover networks and modified data manipulator networks," *Appl. Opt.* **28**(13), 2494–2498 (1989).
14. J. Jahns, "Optical implementation of the Banyan network," *Opt. Commun.* **76**(5,6), 321–324 (1990).
15. T. Yoshimura, S. Tsukada, S. Kawakami, M. Ninomiya, Y. Arai, H. Kurokawa, and K. Asama, "Three-dimensional micro-optical switching system architecture using slab-waveguide-based micro-optical switches," *Opt. Eng.* **42**(2), 439–446 (2003).
16. D. G. Sun, N. X. Wang, L. M. He, M. Xu, G. D. Liang, and J. Zheng, "Research on optical multistage butterfly interconnection and optoelectronic logic operations," *Opt. Laser Technol.* **26**(6), 378–383 (1994).
17. D. G. Sun, N. X. Wang, L. M. He, Z. W. Lu, and Z. H. Weng, "Butterfly interconnection networks and their applications in information processing and optical computing: applications in fast-Fourier-transfor-based optical information processing," *Appl. Opt.* **32**(35), 7184–7193 (1993).
18. R. A. Thompson, "The dilated slipped Banyan switching network architecture for use in an all-optical local-area network," *J. Lightwave Technol.* **9**(12), 1780–1787 (1991).
19. M. M. Vaez and C. T. Lea, "Blocking performance with crosstalk consideration of the photonic suitching networks based on electrooptical directional couplers," *J. Lightwave Technol.* **17**(3), 381–387 (1999).

De-Gui Sun earned his BS degree in geometrical optics and optical engineering from Harbin Institute of Technology of China in 1985. He earned his MS and PhD degrees in optical physics, optoelectronic devices, and applications from Changchun Institute of Optics and Fine Mechanics, Chinese Academy of Sciences of China, in 1988 and 1993, respectively. As a postdoctoral fellow, he worked on research on polymeric waveguide electro-optic (EO) modulators and other EO devices at the Microelectronics Research Center of the University of Texas at Austin from 1994 through 1997. As a technical leader, he joined a startup company in Canada from 1998 through 2001, and worked on the development of passive components. As a research associate, he was also engaged in research on new high-performance EO modulators at Northwestern University, Chicago, Illinois, from 2002 through 2003. Now he is a professor and PhD degree director at the Changchun Institute of Optics, Fine Mechanics, and Physics, Chinese Academy of Sciences of China. His research interests include integrated optoelectronic components, high-performance EO modulators, new optical networks and related technologies, new optical telecommunications systems, and their applications in industry.

Biographies and photographs of other authors not available.